JOURNAL OF AGRICULTURAL AND FOOD CHEMISTRY

Functional and Structural Properties of 2S Soy Protein in Relation to Other Molecular Protein Fractions

SOK LI TAY, STEFAN KASAPIS,* CONRAD O. PERERA, AND PHILIP J. BARLOW

Department of Chemistry, National University of Singapore, Block S3, Level 6, Science Drive 4, Singapore 117543

The purpose of this investigation is to develop a better understanding of the structure−function relationship of the 2S fraction of soy protein that has not been considered in earnest by the research community. Defatted soy flour was used to extract the three major fractions of the protein (2S, 7S, and 11S). It was found that 2S exhibits better foaming and emulsification properties than the other two molecular fractions. Work was extended to structural properties, which were monitored using spectrophotometry, atomic force microscopy, scanning electron microscopy, small-deformation dynamic oscillation on shear, and large-deformation compression testing. An experimental protocol utilizing glucono-δ-lactone (GDL), GDL with *N*-ethylmaleimide, or GDL with urea was capable of identifying the nature of molecular interactions responsible for gelation. Surprisingly, it was found that in the initial stages of structure formation, 2S fared better than 7S, with 11S exhibiting the highest rates of aggregation. Given time, however, 7S produced a firmer network with a better water-holding capacity than that of 2S. Non-covalent interactions, as opposed to disulfide bridging, were found to be largely responsible for the changing functionality of the molecular fractions throughout the experimentation from the formation of a vestigial structure to that of a mature gel.

KEYWORDS: 2S soy protein; structure−function relationship; 7S soy protein; 11S soy protein; foaming; gelation; aggregation; water-holding capactiy

INTRODUCTION

Soy protein is increasingly being used as a functional ingredient in an effort to imitate desirable organoleptic properties in processed food products (*1*). It is advantageous that among legumes, soybean has a high protein content containing three major molecular fractions (11S, 7S, and 2S). The molecular masses of these three fractions are approximately 300, 189, and 18 kDa, with the percentage contents being about 42, 34, and 15%, respectively (*2*). Through the years, research on structure−function relationships has been carried out mainly on 11S and 7S.

With regard to the interfacial studies, 11S was found to be a rather poor emulsifying agent due to the difficulty in adsorbing at the oil−water interface (*3*). This was attributed to the low surface hydrophobicity, low chain flexibility, and high molecular weight of the protein (*4*). Furthermore, Utsumi et al. modified 11S at a molecular level, thus designing recombinant systems in which the extent of hydrophobicity of the C-terminal region would determine largely the emulsifying properties (*5*). In the case of 7S, the extension region found in subunits α and α' possessed the required functionality for good solubility and emulsification.

Gelation induced by glucono-δ-lactone (GDL) has been extensively studied, and Kohyama and Nishinari (*6*) reported that the breaking stress of the 7S gel was smaller than that for 11S. Similarly, the rate of gelation for 7S was lower than that for 11S. In addition, the low isoelectric point of 7S maintained a relatively high pH value in the gel, but the protein possessed lower cohesiveness, gumminess, and lightness than the 11S preparation at 4% solids (*7*, *8*). Scanning electron microscopy (SEM) showed that 11S produced a coarse network with a pore size of 2−3 μm, whereas 7S exhibited a finer structure of $\approx$0.5 μm pore size (*7*). Puppo and Añón (*9*) reported that acidic gels of the two molecular fractions are stabilized by non-covalent bonds, with the contribution of disulfide bridging to network stability becoming prominent only in an alkaline environment. Finally, Mills et al. (*10*) argued that precursors of a three-dimensional structure in the form of insoluble macroaggregates can be captured during thermal denaturation of a dilute solution of 7S (1% solids).

The scarcity of studies dealing with the relationship between structure and functional properties of 2S may be twofold: Clearly, the well-known allergenicity of the albumin family of 2S found in Brazilian nuts did not help to raise an interest in the physicochemical properties of the material (*11*). Thus, several food allergens associated with the protein fraction of 2S obtained from various natural sources (sunflower seed, sesame seed, soybean, etc.) have been reported (for example, the Kunitz trypsin inhibitors in ref *12*). According to Lin et al., however, the extent of allergenicity of the 2S fraction from

* Corresponding author (e-mail chmsk@nus.edu.sg; fax +65 6775 7895; telephone +65 6516 4834).

10.1021/jf060387a CCC: $33.50
Published on Web 07/08/2006

soybean has not been, as yet, rigorously documented (*13*). Another reason is the composition of the soy protein, as 2S is the smallest of the three major fractions (*2*).

Putting the above considerations aside, Burnett et al. reported on the emulsification properties of two variants of 2S from sunflower seed (*14*). Formulations of 11S with 2S from sesame flour were tried as a substitute for traditional uses of dairy and soybean proteins in beverages and were met with an acceptable response from a hedonic sensory evaluation panel (*15*). Sorgentini and Wagner found that whey soy protein, which is made up of a mixture of 2S and 7S fractions, exhibited good foaming capacity within a broad pH range *(*from pH 2 to 10 in ref *16*). The current investigation aims to provide further insights into the surface active, aggregation, and gelation properties of the 2S soy protein, and discusses this profile with the corresponding behavior of the more established molecular counterparts.

MATERIALS AND METHODS

Source and Biochemical Characterization. Soybean belongs to the family Leguminosae (genus *Glycine* L.) (*17*). The defatted soy flour (product code 063-130), used in this investigation to extract the soy protein fractions of 2S, 7S, and 11S, was purchased from Archer Daniels Midland Co. (Decatur, IL). The literature includes extensive data on the characterization of these fractions in terms of primary to quaternary structures, sulfhydryl content, composition and crystal structure of the molecular subunits, biological activity, and nutritional quality (*2*, *7*, *13*, *18*−*20*).

Isolation of the Molecular Soy Protein Fractions. The large molecular weight materials (7S and 11S) were isolated according to the method of Nagano et al. (*21*), whereas the 2S fraction was obtained using the method of Rao and Rao (*22*). All three fractions were dissolved in deionized water and adjusted to pH 7.5 before dialysis with deionized water for 24 h at 4 °C. The final step was followed by freeze-drying. The 6.25 × N conversion factor was used to convert percentage nitrogen (obtained by Kjeldahl) to protein content in the defatted soy fractions.

Measurements of Foaming and Emulsification. Foaming properties were determined as follows: air, at a flow rate of 90 cm^3/min, was introduced into 6 mL of 0.1% protein solution in a graduated column of 10 mm diameter with a coarse glass frit at the bottom. Bubbling was continued for 140 s. The volume of liquid incorporated to the foam was determined by measuring the volume in the liquid remaining in the column (*23*).

The emulsifying properties of the samples were determined as follows: The emulsions, 1.0 mL of corn oil and 3.0 mL of the protein solution (0.2%), were prepared in 0.035 M phosphate buffer at pH 7.6 and were homogenized using an Ultra turrax T18 homogenizer (IKA Works, Wilmington, NC). Homogenization was carried out at 20 °C for 1 min at 18000 rpm. Fifty microliters of the emulsion was taken from the bottom of the container at different time intervals and diluted with 5 mL of a 0.1% sodium dodecyl sulfate solution. The absorbance was determined at 500 nm (*24*). The surface hydrophobicity of the protein sample was estimated according to the method of Rawel et al. (*25*).

Formation of Aggregates. Protein preparations were heated for 10 min at 100 °C and then cooled to 25 °C to form a homogeneous dispersion. Aggregation would occur following the addition of a freshly prepared GDL solution to the system, with the resultant mixture containing protein at 4.0% (w/v) and GDL at 0.4% (w/v). To block the chemical interaction in the aggregates, 10 mM *N*-ethylmaleimide (NEM) was added to the cooled sample an hour prior to the addition of GDL. Physical interactions in the aggregates were inhibited by adding urea (6 M) to the system in accordance with the procedure described for NEM.

Turbidity and Images of the Aggregates. Aggregation during the GDL acidification was determined by measuring the turbidity of 1 mL of the soy sample in a semimicro cuvette as the absorbance at 600 nm and 25 °C using a UV−visible spectrophotometer (Shimadzu model UV 1601, Kyoto, Japan) (*26*). Images of the vestigial structure formation were recorded using atomic force microscopy (AFM) (Veeco Metrology Group Inc., Santa Barbara, CA) (*27*). A drop of sample solution (30 μL) was deposited onto freshly cleaved mica for 4 min. Then argon gas was used to blow dry the samples. These were imaged under ambient conditions with a Multimode AFM connected to a Nanoscope IIIa scanning probe microscope controller. All images were acquired in tapping mode using Veeco Nanoprobe tips (Veeco Metrology Group Inc.).

Scanning Electron Microscopy (SEM). Single 2S, 7S, and 11S gels containing 4.0% (w/v) protein and 0.4% (w/v) GDL were left to age at room temperature (25 °C) for 24 h prior to experimentation. Next, samples were deep frozen in liquid nitrogen and freeze-dried. Materials were fixed to a stub and coated with platinum using a sputter coater (JEOL model JFC-1300, Tokyo, Japan). Networks were observed using SEM, which operated at an accelerating voltage of 15 kV (JEOL model JSM-5600LV).

Water-Holding Capacity (WHC). Gels were acidified and aged according to the procedure of the preceding paragraph. Then, they were placed on a 50 mL Maxi-Spin centrifuge tube with a plain nylon membrane (4.5 μm) in the middle position (Vivascience AG, Hanover, Germany) and centrifuged at 120*g* for 5 min at 15 °C. WHC was expressed as the percentage of water remaining in the gel after centrifugation.

Rheological Measurements. Gels similar to those used for SEM and WHC analyses were subjected to large-deformation compression testing. Work focused on the hardness (or apparent breaking stress) of the gels, which was determined by compressing cylindrical disks of 15 mm diameter and 10 mm height to 80% of their original height (*28*). A 35 mm diameter probe in a TA.XT2i texture analyzer (Stable Microsystems, Godalming, Surrey, U.K.) was employed, and the compression rate was 0.1 mm/s. Temperature was ambient.

Small-deformation mechanical measurements on shear were performed with the Advanced Rheometrics Expansion System (ARES), which is a controlled strain rheometer (Rheometric Scientific, Piscataway, NJ). A parallel-plate geometry of 50 mm diameter and 1 mm gap was used. Samples were prepared as described under Formation of Aggregates and loaded onto the platen of the rheometer, and their exposed edges were covered with a silicone fluid from BDH (100 cS) to minimize water loss. These were subjected to an isothermal run (25 °C) for up to 24 h at the frequency of 1 rad/s. The time sweep was followed by a frequency sweep between 0.1 and 100 rad/s. In both cases, a strain within the linear viscoelastic region was used (0.1%). The experimental protocol provides readings of the storage modulus (G'; elastic component of the network) and loss modulus (G''; viscous component) and a measure of the "phase lag" δ ($\tan \delta = G''/G'$) of the relative liquid-like and solid-like character of the material (*29*).

Statistical Analysis and Support of Results. Three to four replicates per reading were used for the statistical analysis of foaming and emulsification properties, pH variation following GDL addition, and solution turbidity measured as absorbance at 600 nm. Thus, in **Figures 1**, **2**, **4**, and **6** data points represent the mean value of a series of measurements, with the error bars indicating the spread of the observations in terms of one standard deviation. Comparison of the mean values of these measurements recorded for two experimental preparations was carried out by the paired *t* test with a significance level of $P < 0.05$. Comparisons of variance for the means of more than two samples were carried out by the single-factor ANOVA. For example, all readings in **Figure 6a** are not significantly different, whereas those in **Figure 6b** are significantly different on the basis of the single-factor ANOVA. Outcomes of the statistical analysis were taken into account in the discussion of experimental results assessing the distinctiveness of profiles recorded for 2S in comparison with those of 11S and 7S. With regard to the small-deformation mechanical measurements in **Figure 7**, triplicate runs of different preparations yielded effectively overlapping traces, thus reproducing the process of gelation as a function of time scale of observation following GDL addition within a 2% error margin.

RESULTS AND DISCUSSION

Foaming and Emulsification Properties. The air and water phases in foams form a thermodynamically unstable system due

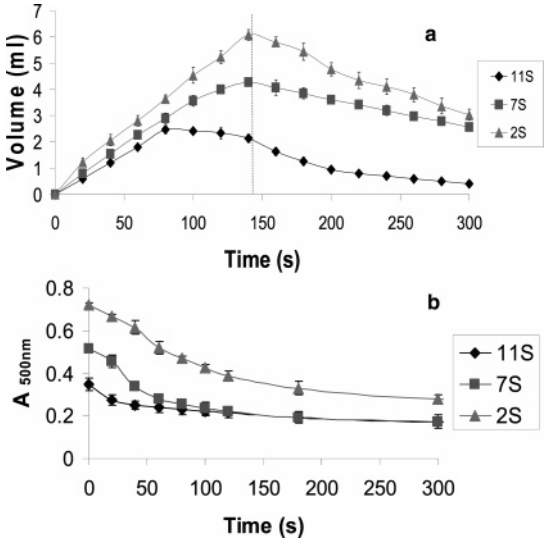

Figure 1. Interfacial behavior of the three soy protein fractions, that is, 11S, 7S, and 2S, as demonstrated for (**a**) the foaming and (**b**) the emulsifying properties.

to unfavorable interactions at the interface and the different densities of the two domains. **Figure 1a** reproduces the profiles of foam formation and subsequent destabilization in our soy fractions following air injection to solutions for up to 140 s. To the left of the dotted line, the curve indicates foam formation. In this context, stable foam formation relates to an increasing volume of water being incorporated into the biphasic system. On the right side of the dotted line, the drop in the profile of volume development as a function of time reflects the destabilization of the foam, which will eventually collapse due to liquid drainage.

The maximum volumes of water (V_{max}) incorporated in the foams of 2S, 7S, and 11S are 6.1, 4.4, and 2.5 mL, respectively. Thus, 2S is able to take in the highest amount of water, a result that argues for the protein forming the best adsorption medium in the air/water interface. The relatively poor foaming performance of 11S is highlighted because the V_{max} value is obtained early within the air injection period (80 s in **Figure 1a**). The stability of the foam beyond air injection is also of interest and, in the present context, this is defined as the time of half-drainage of water that was incorporated in the foam after 140 s ($t_{1/2}$) (*23*). As for the foam creation, 11S exhibits the least stability, with the value of $t_{1/2}$ being 60 s, as compared with the 2S and 7S air/water structures ($t_{1/2} \approx 160$ s).

Next, the emulsification properties of the soy protein fractions were examined. This was assessed from the turbidity of the emulsion, because reduction of the oil/water interface tension and suspension of the oil droplets by the continuous aqueous phase leads to an increase in turbidity (*30*). In **Figure 1b**, the absorbance values, which indicate the turbidity level of the emulsions formed by the 2S, 7S, and 11S at time zero, are 0.72, 0.51, and 0.35, respectively. Once more, 2S was found to possess better functional properties (stabilization of the oil droplets against coalescence this time round) as compared to the higher molecular weight counterparts. The fraction corresponds to the least percentage composition of the soybean protein, but possesses attractive foaming and emulsification characteristics that render weight to potential applications as a single functional ingredient or a tailor-made addition to a protein composite.

To rationalize the above results, one should consider that protein-supported interfacial processes involve rapid diffusion

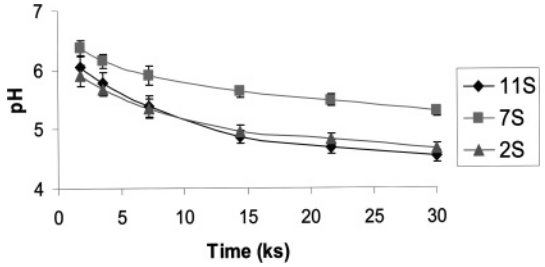

Figure 2. pH variation as a function of time following GDL addition at ambient temperature for the three soy protein fractions.

of the macromolecule to the air/water or oil/water interface, adsorption, and reorientation to form a film leading to reduction in the interfacial tension (*31*). It has been demonstrated that the higher the hydrophobicity of a protein fraction, the more stable the film that forms at the air/water interface (*16*). Furthermore, the gradient of the fluorescence intensity versus protein concentration can be used as an index of surface hydrophobicity, which relates reasonably well to structural properties (H_0) (*3*, *32*). Following this approach, the present work found that 11S exhibits the least hydrophobic character ($H_0 = 388$) among the soya fractions (H_0 for 2S is 483 and 446 for 7S) at neutral pH.

The relationship between fluorescence intensity/surface hydrophobicity and structural properties identified presently for soy proteins ties well with reasoned ideas found in the literature. Thus, it has been proposed that the poor surface active properties of 11S are due to the inability of intra- and intersubunit disulfide bonds to undergo rapid rearrangement at the interface, which could expose hydrophobic regions to the oil phase (*3*, *33*). Instead, the hydrophobic "basic" subunits of 11S are located predominantly in the interior of the molecule, whereas the more hydrophilic "acid" subunits remain at the outside of the molecule (*34*). The structural properties of the molecular fraction can be improved at acidic or high alkaline pH and with increasing temperature, leading to unfolding or dissociation into smaller subunits with higher surface hydrophobicity (*35*, *36*). In terms of the 2S fraction, there is a report on the emulsification properties of albumins from sunflower seed (*14*). FT-IR measurements indicate changes in the secondary structure once adsorbed to the oil/water interface and the presence of intermolecular β-sheets with a considerable component of hydrophobic patches. Therefore, interfacial adsorption at a definite orientation that maximizes the contacts between the nonpolar groups appears to be the underlying mechanism determining the surface active characteristics of 2S.

Aggregation of the Molecular Fractions. Soy protein is a texture modifier and, as such, the phase viscosity increases through the gradual buildup of aggregates, which may lead eventually to the formation of a continuous gelled phase. The remaining part of this discussion focuses primarily on the development of structure in our molecular fractions and its rationalization. A starting point to consider is the change in pH with time due to addition of GDL. **Figure 2** reproduces the gradual increase in the acidity of the three protein fractions following addition of the acidifier, which hydrates slowly to form gluconic acid. Upon standing for 30 ks, a noticeable drop in pH values is recorded ranging from 5.3 to 4.67 and 4.53 for the 7S, 2S, and 11S gels, respectively. Clearly, 7S exhibits the best buffering capacity against the added protons, as opposed to those of 2S and 11S, which are comparable. This information will prove to be useful in the examination of the effect of generated acidity on structure formation.

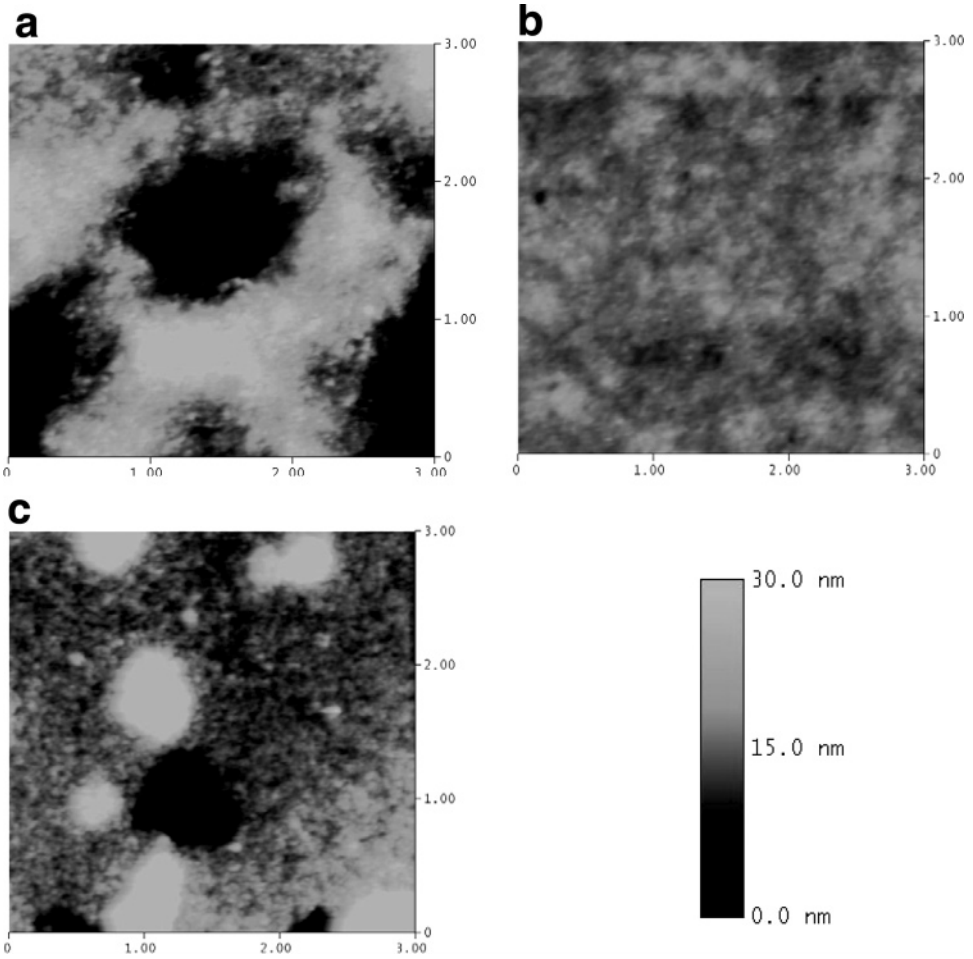

Figure 3. AFM images of the three types of soy protein aggregates [(**a**) 11S, (**b**) 7S, and (**c**) 2S] following the addition of 0.4% GDL and deposition onto mica for 4 min (scan size = 3 μm by 3 μm).

Both AFM and spectrophotometry are particularly suited for the capture of vestigial structure in the time domain (*27*). In **Figure 3a**, the white tracks, which contrast strongly with the black featureless background, represent domains of an intense aggregate buildup. This takes place within 4 min of adding GDL to the solution of 11S at ambient temperature. It appears that the fraction exhibits rapid kinetics of aggregation. Despite the addition of GDL, the aggregation process of 7S is slow and cluster formation remains rather sporadic within the time frame of experimental observation (**Figure 3b**). 2S forms intermediate-size structures, which are imaged as white discontinuous inclusions in the viscous suspension (**Figure 3c**). Clearly, the rate of the aggregation process is governed by the extent of acidification discussed in **Figure 2**, with the most acidic environment of 11S and 2S being conducive to the development of a proteinacious structure.

Semiquantitative confirmation of the relative patterns in structure development can be obtained from turbidity measurements at ambient temperature. Increase in turbidity, owing to buildup of aggregation, is reflected in the values of absorbance (*A*), which presently are recorded at 600 nm to eliminate potential chromophoric complications from molecular groups at lower wavelengths. There is an early increment in readings for 11S, which reach a plateau at 2.5 ks (**Figure 4a**). This is followed by 2S and 7S achieving constant levels at 15 and 24 ks, respectively. Thus, the degree of protein aggregation unveiled in the micrographs of the preceding paragraph is consistent with the order of turbidity development using spectrophotometry.

The isoelectric point (p*I*) of 11S is 6.4, followed by 7S (4.8) and 2S (4.5) (*37*). Solely on the basis of the effect of p*I* and for the same pH value, the extent of aggregation of the three molecular fractions following GDL addition should be in the order 11S > 7S $\approx$ 2S. However, the actual buffering capacity was found to create the distinct sequence of 11S > 2S > 7S, with the 2S exhibiting three-dimensional formations earlier than expected. Clearly, simple p*I* considerations are not adequate to rationalize the experimental trend, and factors such as the nature and extent of intermolecular forces responsible for structure development should now be considered.

The prevailing type of interactions in soy protein was probed with urea and NEM. The former is well-known to destabilize forces of a secondary nature, that is, hydrophobic, electrostatic, and hydrogen bonding (*38*). As shown in **Figure 4b**, addition of urea has an adverse effect on the kinetics of vestigial structure formation for all fractions, but the aggregation profile of 11S recovers fully during the isothermal run. In the case of 7S and 2S, there is an irreversible loss in molecular functionality, with the values of absorbance leveling off well below those recorded in the absence of the reagent. Urea preserves chemical interactions in the system and, in **Figure 4b**, these create the following order of structure formation: 11S > 2S $\approx$ 7S. However, this outcome is not congruent with the overall response observed in **Figure 4a**.

NEM, on the other hand, is used to block chemical interactions in the nature of the thiol groups (*39*). Gratifyingly, NEM addition to soy preparations in **Figure 4c** yields aggregation rates that are effectively identical to those first recorded in **Figure 4a**. This result argues convincingly for the absence of

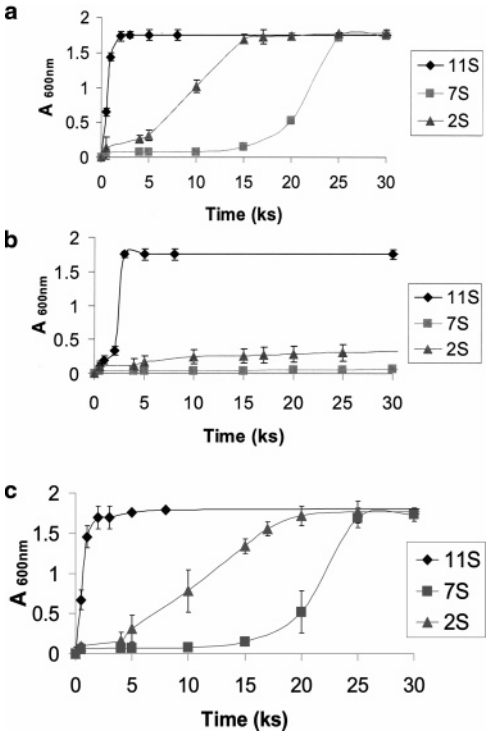

Figure 4. Absorbance readings at 600 nm due to the development of turbidity in the three types of soy protein aggregates following GDL addition: (**a**) overall profile; (**b**) in the presence of urea; (**c**) in the presence of NEM.

thiol group contributions to structure at the vestigial stage. Physical interactions survive in the presence of NEM and create the descending order 11S > 2S > 7S also noted in the absence of reagents, thus rendering the effect of p*I* and thiol groups secondary in early aggregation.

Formation of Three-Dimensional Structures upon Aging. A preliminary exploration of the structural features of soy preparations included the WHC and rapid compression testing. In doing so, samples were left to age for 80 ks at ambient temperature. WHC examination at the end of the standing period yielded the following results: 11S gel, 70.1%; 7S, 64.4%; and 2S, 42.2%. Compression testing focused on the force required to fracture the gel (hardness or apparent breaking stress), thus producing values of 4.4, 2.4, and 0.8 kPa with decreasing molecular mass distribution of the macromolecules in the soy network. It is clear, at this point, that the gel hardness and WHC properties exhibit a common pattern of functionality according to the order 11S > 7S > 2S. These basic features of the soy network are not related directly to the kinetics of aggregate formation earlier examined, at which the 2S exhibited accelerated functionality.

Further confirmation of the incongruity between the overall trend in the aggregation profile and the final rate of gelation in the soy protein fractions is presented by means of SEM. **Figure 5a** illustrates a well-developed, "honeycomb" structure obtained for the mature 11S gel at ambient temperature following addition of GDL. By comparison, the three-dimensional arrangement of 7S appears to include a high number of cavities with a broad size distribution (**Figure 5b**). The imperfections in the organization of the layers of 7S should be responsible for the formation of soft gels, with WHC properties being inferior to those of 11S. Both 11S and 7S, however, form networks with contour-length pores that are able to trap water molecules effectively in comparison with the 2S gel. Thus, extensive structural defects are noted in the three-dimensional image of the 2S network, resulting in a poor WHC and the softest intermolecular assembly (**Figure 5c**).

The unexpected deterioration in the functionality of the aged 2S gel needs also to be explained. To understand the gelation process, once more, we employed the interplay between the formation of chemical gels, where cross-linking is covalent, and physical gels, which contain non-covalent cross-links. **Figure 6a** reproduces the development of turbidity recorded between 30 and 80 ks, following GDL addition, and at the remaining experimental conditions described earlier for shorter time periods of observation (0−30 ks in **Figure 4**). For all fractions, a plateau is obtained at a single reading of absorbance, an outcome which signifies the formation of an "infinite" network of molecules, that is, macroscopic in size, so that its turbidity characteristics exceed the maximum reading capacity of the signal detector of the instrument.

With regard to the addition of chemical reagents, a single spectroscopic response identical to that in **Figure 6a** is recorded for the three soy fractions in the presence of NEM (results not shown here). However, the behavior of our systems changes considerably once urea eliminates the physical contributions to network stability. Thus, in **Figure 6b**, 11S cross-links appear to be affected the least by this environment, but the 7S network is severely disrupted. The molecular structure of 2S is rather different from that of 7S and involves some contributions from thiol groups, with the overall profile of the underlying "gel state" in the presence of urea being 11S > 2S > 7S. These results are, of course, at variance with the WHC, textural, and structural properties reported in this section, thus emphasizing the importance of physical associations in the development of the mature 7S network.

Complementary evidence that the morphology of our networks is quite distinct from that of chemical gels and that physical forces predominate in the long-distance scales of molecular interactions is probed by rheological, particularly viscoelastic, experiments (*40*). This approach is invaluable in the context of the present investigation for making measurements on aged gels that are not subject to "upper bound" limitations in readings seen for spectroscopy in **Figure 6a**. Thus, gel cure experiments of the soy preparations were carried out in real time using small-deformation oscillatory rheometry. The pregelled system (in the fluid state) was loaded onto a parallel plate assembly at ambient temperature, and one of the plates was oscillated at a fixed frequency and fixed maximum strain. As the gel begins to "set up", readings of G' and G'' are recorded for 80 ks to match the time scale of observation employed in spectroscopy experiments.

Figure 7 reproduces the characteristic time profile of gelation obtained for the three soy fractions at the concentration of 4% and in the presence of GDL. To avoid clutter, only the G' trace is illustrated. Materials exhibit a pasty viscoelasticity with a solid-like response; that is, values of the storage modulus predominate over those of the loss modulus, with the damping factor, tan δ, being just below 0.1. There is a rapid development in the elastic component of the 11S network, which achieves an apparent equilibrium modulus of $\approx$1 kPa relatively early within the time run (5 ks). The cold-setting behavior of 7S is considerably slower but, overall, it forms a sigmoidal modulus−time profile indicative of co-operative gelation. In contrast, 2S exhibits a progressive increase in the values of G', which appear to level off at $\approx$60 ks. The values of G' of the 2S network are substantially lower than for the two remaining counterparts, never exceeding 50 Pa (log $G' = 1.7$). Finally, addition of NEM

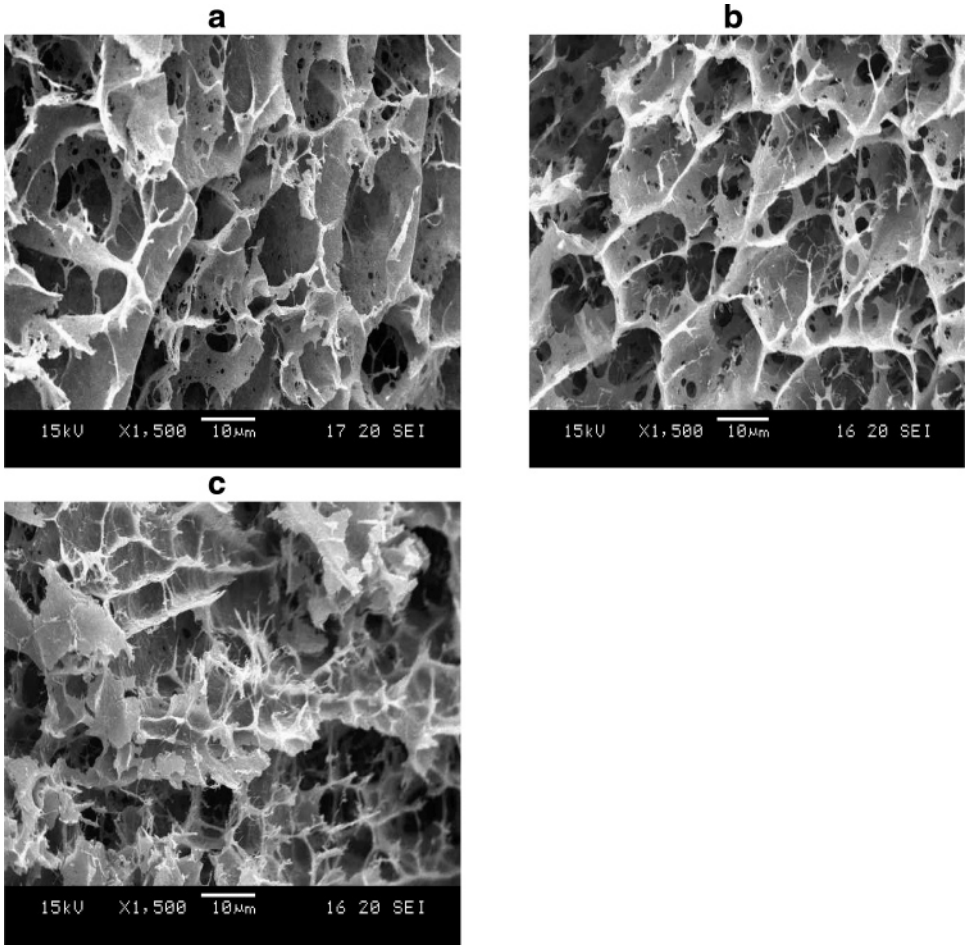

Figure 5. SEM images of the three types of soy protein gels: (**a**) 11S; (**b**) 7S; (**c**) 2S (magnification, 1500×).

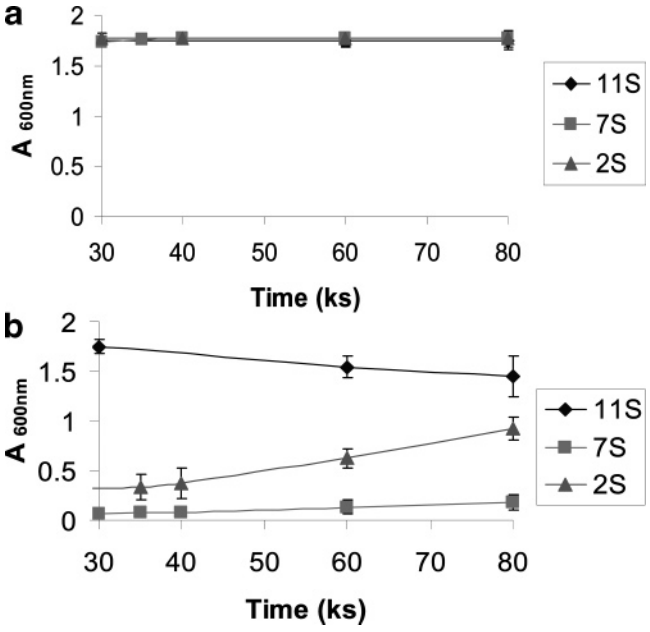

Figure 6. Absorbance readings at 600 nm due to the development of turbidity in the three types of soy protein gels following GDL addition: (**a**) overall profile; (**b**) in the presence of urea.

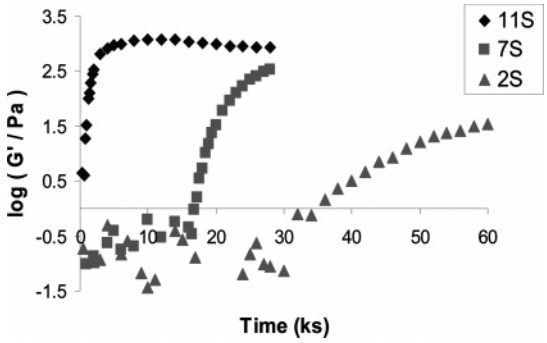

Figure 7. Time course of *G′* for the three soy fractions at 25 °C, frequency of 1 rad/s, and strain of 0.1%.

produced a mechanical response qualitatively similar to that of **Figure 7**, whereas in the presence of urea, aggregate formation was unable to create a sufficient volume of intermolecular interactions for the formation of cohesive three-dimensional structures within the experimental time scale of observation (results not shown).

Concluding Remarks. The present paper explores the functional and structural features of the 2S soy protein and then compares them with the corresponding properties of the high molecular mass counterparts (11S and 7S). **Figure 1** shows the enhanced ability of the native 2S soy protein to hold water at interfaces, a result that should be attributed to the high surface hydrophobicity and chain flexibility of the low molecular mass chains of the material. Protein concentrations of the three molecular fractions in these studies were kept low, that is, between 0.1 and 0.2% in the solution. It can be argued that, on the basis of the superior interfacial properties of the native 2S soy protein, its inclusion in a variety of food products may improve their foaming and emulsification performances.

A much higher concentration is required for the gelation of the thermally denatured soy protein fractions, which in the present study is 4% (plus 0.4% GDL). Thermal denaturation and addition of GDL result in levels of acidity that do not follow the conventional pattern dictated by the isoelectric point of the three molecular fractions. Thus, GDL-strengthened 2S systems exhibit unexpected signs of an early aggregation owing to noncovalent interactions (**Figure 4**). However, further curing of the material at ambient temperatures results in soft gels (**Figure 7**) with an inferior three-dimensional structure (**Figure 5**) and WHC compared to the remaining two proteinaceous fractions. The low molecular mass of the 2S chains is now a disadvantage with regard to the gelation properties. Together, these two types of experimentation, that is, nonthermal/native and denatured/GDL, constitute a sharp contrast in the structure−function relationship of the 2S soy protein.

LITERATURE CITED

(1) Nunes, M. C.; Batista, P.; Raymundo, A.; Alves, M. M.; Sousa, I. Vegetable proteins and milk puddings. *Colloids Surf. B: Biointerfaces* **2003**, *1*, 1−9.

(2) Fukushima, D. Recent progress of soybean protein foods: chemistry, technology, and nutrition. *Food Rev. Int.* **1991**, *7*, 323−351.

(3) Rickert, D. A.; Johnson, L. A.; Murphy, P. A. Functional properties of improved glycinin and β-conglycinin fractions. *J. Food Sci.* **2004**, *69*, 303−311.

(4) Wagner, J. R.; Guéguen, J. Effects of dissociation, deamidation, and reducing treatment on structural and surface active properties of soy glycinin. *J. Agric. Food Chem.* **1995**, *43*, 1993−2000.

(5) Utsumi, S.; Maruyama, N.; Satoh, R.; Adachi, M. Structure−function relationships of soybean proteins revealed by recombinant systems. *Enzyme Microb. Technol.* **2002**, *30*, 284−288.

(6) Kohyama, K.; Nishinari, K. Rheological studies on the gelation process of soybean 7S and 11S proteins in the presence of glucono-δ-lactone. *J. Agric. Food Chem.* **1993**, *41*, 8−14.

(7) Kohyama, K.; Murata, M.; Tani, F.; Sano, Y.; Doi, E. Effects of protein composition on gelation of mixtures containing soybean 7S and 11S globulins. *Biosci., Biotechn., Biochem.* **1995**, *34*, 240−245.

(8) Tay, S. L.; Perera, C. O. Effects of glucono-δ-lactone on 7S, 11S proteins and their protein mixture. *J. Food Sci.* **2004**, *6*, 139−143.

(9) Puppo, M. C.; Añón, M. C. Structural properties of heat-induced soy protein gels as affected by ionic strength and pH. *J. Agric. Food Chem.* **1998**, *46*, 3583−3589.

(10) Mills, E. N. C.; Huang, L.; Noel, T. R.; Gunning, P., Morris, V. J. Formation of thermally induced aggregates of the soya globulin β-conglycinin. *Biochim. Biophys. Acta* **2001**, *1547*, 339−350.

(11) Nordlee, J. A.; Taylor, S. L.; Townsend, J. A.; Thomas, L. A.; Bush, R. K. Identification of a brazil nut allergen in transgenic soybeans. *N. Engl. J. Med.* **1996**, *334*, 688−692.

(12) Moroz, L. A.; Yang, W. H. Kunitz soybean trypsin inhibitor: a specific allergen in food anaphylaxis. *N. Engl. J. Med.* **1980**, *301*, 1126−1128.

(13) Lin, J.; Fido, R.; Shewry, P.; Archer, D. B.; Alcocer, M. J. C. The expression and processing of two recombinant 2S albumins from soybean (*Glycine max*) in the yeast *Pichia pastoris*. *Biochim. Biophys. Acta* **2004**, *1698*, 203−212.

(14) Burnett, G. R.; Rigby, N. M.; Mills, E. N. C.; Belton, P. S.; Fido, R. J.; Tatham, A. S.; Shewry, P. R. Characterization of the emulsification properties of 2S albumins from sunflower seed. *J. Colloid Interface Sci.* **2002**, *247*, 177−185.

(15) Lopez, G.; Flores, I.; Galvez, A.; Quirasco, M.; Farres, A. Development of a liquid nutritional supplement using a *Sesamum indicum* L. protein isolate. *Lebensm.-Wiss. -Technol.* **2003**, *36*, 67−74.

(16) Sorgentini, D. A.; Wagner, J. R. Comparative study of foaming properties of whey and isolate soybean protein. *Food Res. Int.* **2002**, *35*, 721−729.

(17) Clarke, E. J.; Wiseman, J. Developments in plant breeding for improved nutritional quality of soya beans I. Protein and amino acid content. *J. Agric. Sci.* **2000**, *134*, 111−124.

(18) García, M. C.; Torre, M.; Marina, M. L.; Laborda, F. Composition and characterization of soybean and related products. *Crit. Rev. Food Sci. Nutr.* **1997**, *37*, 361−391.

(19) Maruyama, N.; Adachi, M.; Takahashi, K.; Yagasaki, K.; Kohno, M.; Takenaka, Y.; Okuda, E.; Nakagawa, S.; Mikami, B.; Utsumi, S. Crystal structures of recombinant and native soybean β-conglycinin β homotrimers. *Eur. J. Biochem.* **2001**, *268*, 3595−3604.

(20) Adachi, M.; Kanamori, J.; Masuda, T.; Yagasaki, K.; Kitamura, K.; Mikami, B.; Utsumi, S. Crystal structure of soybean 11S globulin: glycinin A3B4 homohexamer. *Proc. Natl. Acad. Sci. U.S.A.* **2003**, *100*, 7395−7400.

(21) Nagano, T.; Hirotsuka, M.; Mori, H.; Kohyama, K.; Nishinari, K. Dynamic viscoelastic study on the gelation of 7S globulin from soybeans. *J. Agric. Food Chem.* **1992**, *40*, 941−944.

(22) Rao, A. G. A.; Rao, M. S. N. A method for isolation of 2S, 7S and 11S proteins of soybean. *Preparative Biochem.* **1977**, *7*, 89−101.

(23) Molina, O. S. E.; Wagner, J. R. Hydrolysates of native and modified soy protein isolates: structural characteristics, solubility and foaming properties. *Food Res. Int.* **2002**, *35*, 511−518.

(24) Pearce, K. N.; Kinsella, J. E. Emulsifying properties of proteins: evaluation of a turbidometric technique. *J. Agric. Food Chem.* **1978**, *26*, 716−723.

(25) Rawell, H. M.; Czajka, D.; Rohn, S.; Kroll, J. Interactions of different phenolic acids and flavonoids with soy protein. *Int. J. Biol. Macromol.* **2002**, *30*, 137−150.

(26) Molina, M. I.; Wagner, J. R. The effects of divalent cations in the presence of phosphate, citrate and chloride on the aggregation of soy protein isolate. *Food Res. Int.* **1999**, *32*, 135−143.

(27) Tay, S. L.; Xu, G. X.; Perera, C. O. Aggregation profile of 11S, 7S and 2S coagulated with GDL. *Food Chem.* **2005**, *91*, 457−462.

(28) Tsoga, A.; Kasapis, S.; Richardson, R. K. The rubber-to-glass transition in high sugar agarose systems. *Biopolymers* **1999**, *49*, 267−275.

(29) Kasapis, S. Definition of a mechanical glass transition temperature for dehydrated foods. *J. Agric. Food Chem.* **2004**, *52*, 2262−2268.

(30) Diftis, N.; Kiosseoglou, V. Improvement of emulsifying properties of soybean protein isolates by conjugation with carboxymethyl cellulose. *Food Chem.* **2003**, *81*, 1−6.

(31) German, J. B.; Phillips, L. Protein interactions in foams: protein−gas-phase interactions. In *Protein Functionality in Food Systems*; Hettiarachchy, N. S., Ziegler, G. R., Eds.; Dekker: New York, 1994; pp 181−208.

(32) Wu, S. W.; Murphy, P. A.; Johnson, L. A.; Fratzke, A. R.; Reuber, M. A. Pilot plant fractionation of soybean glycinin and β-conglycinin. *J. Am. Oil Chem. Soc.* **1999**, *76*, 285−293.

(33) Mitidieri, F. E.; Wagner, J. R. Coalescence of o/w emulsions stabilized by whey and isolate soybean proteins. Influence of thermal denaturation, salt addition and competitive interfacial adsorption. *Food Res. Int.* **2002**, *35*, 547−557.

(34) Lakemond, C. M. M.; de Jonghn, H. H. J.; Hessing, M.; Gruppen, H.; Voragen, A. G. J. Soy glycinin; influence of pH and ionic strength on solubility in relation to molecular structure at ambient temperatures. *J. Agric. Food Chem.* **2000**, *48*, 1991−1995.

(35) Wagner, J. R.; Guéguen, J. Surface functional properties of native acid-treated, and reduced soy glycinin. 2. Emulsifying properties. *J. Agric. Food Chem.* **1999**, *47*, 2181−2187.

(36) Martin, A. H.; Bos, M. A.; Vliet, T. V. Interfacial rheological properties and conformational aspects of soy glycinin at the air/water interface. *Food Hydrocolloids* **2002**, *16*, 63−71.

(37) Dreau, D.; Larre, C.; Lalles, J. P. Semi-quantitative purification and assessment of the purity of the three soybean proteins—glycinin, β-conglycinin and α-conglycinin—SDS-PAGE electrophoresis, densitometry and immunoblotting. *J. Food Sci. Technol.* **1994**, *31*, 489−493.
(38) Chronakis, I. S.; Kasapis, S.; Richardson, R. K. Characterisation of a commercial soy isolate by physical techniques. *J. Texture Stud.* **1995**, *26*, 371−389.
(39) Alting, A. C.; Hamer, R. J.; de Kruif, C. G.; Paques, M.; Visschers, R. W. Number of the thiol groups rather than the size of the aggregates determines the hardness of cold set whey protein gels. *Food Hydrocolloids* **2003**, *17*, 469−479.
(40) Tabilo-Munizaga, G.; Barbosa-Canovas, G. V. Rheology for the food industry. *J. Food Eng.* **2005**, *67*, 147−156.

Received for review February 8, 2006. Revised manuscript received May 1, 2006. Accepted June 2, 2006.

JF060387A